

# Synthesis and modification of 7-aryl derivatives of 4,7-dihydro-[1,2,4]triazolo-[1,5-a]-pyrimidine as potent inhibitors of sirtuin-2

*K. I. Marchenko, A. V. Kyrychenko, N. M. Kolos*

V.N. Karazin Kharkiv National University, 4 Svobody Sq.,  
Kharkiv, 61022, Ukraine

*Received March 31, 2024*

Sirtuin-2 (SIRT2) is a member of the human sirtuin class that regulates various biological processes and is considered a novel biomarker for numerous types of cancer. Depending on the type of tumor, SIRT2 knockout leads to a controversial role in tumorigenesis. However, pharmacological inhibition of SIRT2 with small molecules leads exclusively to inhibition of the growth of many cancer cells, thus opening the way to the therapy of oncological diseases. In this work, we synthesized 7-aryltriazolo[1,5-a]pyrimidine derivatives (some of which showed good inhibitory activity) and modified the active functional groups of the bicyclic structure. The effect of functionalization of the nitrogen atom and the influence of the oxidation and reduction of the dihydropyrimidine fragment on the inhibitory activity of the studied derivatives against sirtuin-2 was analyzed by molecular docking calculations.

**Keywords:** sirtuin-2, inhibitor, organic synthesis, triazolo[1,5-a]pyrimidine, molecular docking.

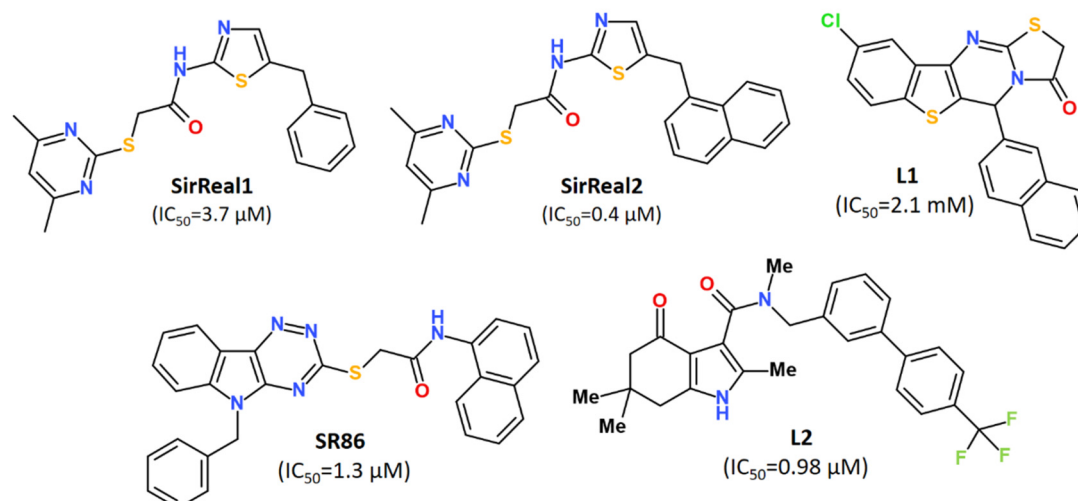
**Синтез і модифікація 7-аройлпохідних 4,7-дигідро[1,2,4]триазоло-[1,5-а]піримідину як потенційних інгібіторів сіртуїну-2.** *К.І. Марченко, О.В. Кириченко, Н.М. Колос.*

Сіртуїни-2 (SIRT2) є представником класу сіртуїнів людини, який регулює різні біологічні процеси та вважається новим біомаркером для різних видів раку. В залежності від типу пухлини, нокаут SIRT2 приводить до суперечливої ролі в пухлиногенезі, однак фармакологічне інгібування SIRT2 малими молекулами веде виключно до пригнічення росту багатьох типів ракових клітин, відкриваючи таким чином шлях до лікування онкологічних захворювань. В цій роботі нами синтезовано ряд похідних 7-аройлтриазоло[1,5-а]піримідину (окремі представники яких показали хорошу інгібуючу активність) та проведена модифікація активних функціональних груп біциклічної структури. З використання молекулярного докінгу було проаналізовано вплив функціоналізації атома нітрогену, окислення та відновлення дигідропіримідинового фрагмента у досліджуваних похідних на процес інгібування сіртуїнів-2.

## 1. Introduction

Silent Information Regulator 2 (SIRT2)-type proteins belong to NAD<sup>+</sup>-dependent protein deacetylases, acting as key regulators of gene expression, DNA repair, cell cycle control, and cell survival [1-2]. Similar to the other members of the Sirtuin family, they have been found in many tissues. However, their highest concen-

trations are observed in the brain and muscle [3]. SIRT2 deacylation targets increase the sensitivity of cells to insulin, as well as the number of mitochondria in the cell and the expression of the antioxidant enzyme, thereby reducing the level of reactive oxygen species [4]. In addition, SIRT2 plays a vital role in oncogenesis: it can either inhibit or promote tumor growth. It



Scheme 1. Representative inhibitors of SIRT2 and their inhibitory activity shown in the brackets.

was shown that SIRT2 acts as tumor suppressors and oncogenes, as well as plays a key role in the invasion and formation of metastases of malignant neoplasms by increasing the cellular motility of cancer cells [5-9]. At the same time, specific SIRT2 inhibitors show high antitumor activity [10-13]. The activity of Sirtuins is inhibited by nicotinamide, which binds to the site of a specific receptor [4, 9]. For this reason, it is known that those drugs that interfere with this association may enhance the natural biological activity of Sirtuins. Developing new agents (small molecules) that specifically block the nicotinamide binding site can become a therapeutic strategy for developing new agents for treating such degenerative diseases as cancer, Alzheimer's disease, diabetes, atherosclerosis, and gout [10, 13].

To date, several types of important Sirtuin-2 inhibitors are known. Among them are open and cyclic peptides, indoles, derivatives of oxadiazole, pyrimidine [14-16], benzimidazole, benzofuran, purine, etc. (Scheme 1). Some peptide inhibitors have been proposed for preclinical studies. SirReal2 is commercially available. A common feature of most potentially inhibitory active compounds, although not always, is the presence of amide groups [17].

Considering the importance of developing novel SIRT2 inhibitors, we synthesized a series of [1,2,4]triazolo[1,5-a]pyrimidine derivatives, which contain promising pyrimidine scaffolds [17]. The inhibitory activity, binding mechanism, and energetics of the synthesized derivatives towards human SIRT2 were examined by molecular docking calculations.

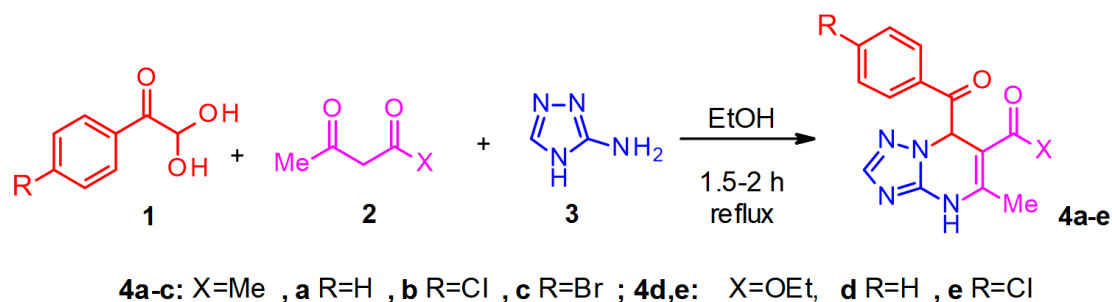
## 2. Experimental

**Reagents and Analytics.** All commercially available reagents and solvents were purchased from commercial vendors and used without purification.  $^1H$  NMR spectra were recorded on a Bruker Avance-300 (300 MHz) spectrometer in DMSO- $d_6$  or  $CDCl_3$  with TMS as an internal reference. Elemental analyses were carried out on an EA 3000 Eurovector elemental analyzer. Melting points were determined on a Melting Point Meter KSP1D. High-resolution mass spectra (electrospray ionization) were recorded using a Dionex Ultimate 3000 liquid chromatograph with a Thermo scientificQ Exactive Plus high-resolution mass spectrometry detector with quadrupole orbitrap. The progress of reactions was monitored by TLC on TLC Silica gel 60 F254 plates (Merck), eluent EtOAc (Merck, analytical grade), visualization under UV light.

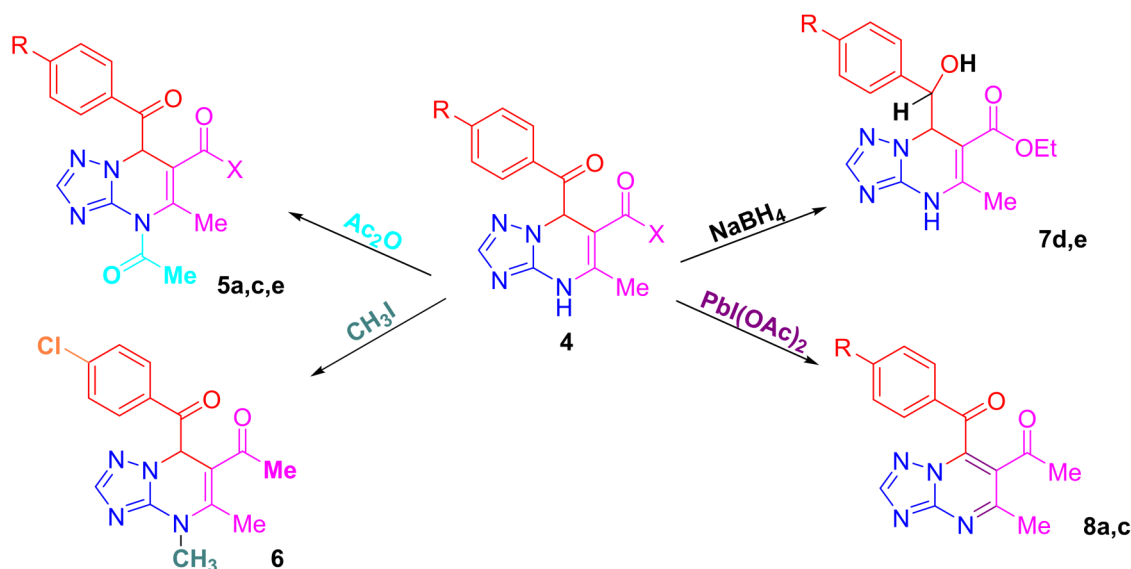
Compounds **4a-e** were synthesized by three component condensation of arylglyoxal hydrate **1**, acetylacetone **2a** or acetoacetic ester **2b**, and 3-amino-1,2,4-triazole **3** according to Scheme 2.

The synthesis of [1,2,4]triazolo[1,5-a]pyrimidine derivatives was previously developed in our lab [18]. In this study, the range of triazolopyrimidines was expanded, and their structure modification was performed. The yields of compounds **4a-e** ranged from 67 to 89%. In most cases, the synthesized products did not require additional purification after separation from the reaction mixture.

The structure of the synthesized compounds **4a-e** contains some functional groups capable



Scheme 2. Synthesis of [1,2,4]triazolo[1,5-a]pyrimidine derivatives.



Scheme 3. Modification of [1,2,4]triazolo[1,5-a]pyrimidine derivatives (see Scheme 2 for more detail)

of further modifications. It was shown that the methylation of triazolopyrimidine **4b** with the participation of methyl iodide in the presence of KOH in acetonitrile does not lead to the formation of the target product. At the same time, the reaction in the NaH-DMF system in an inert medium made it possible to obtain compound **6** in 67% yield. Acylation with acetic anhydride in pyridine was not specific and made it possible to obtain amides **5a,c,e**. Reduction of the 7-aryl group with sodium borohydride in methanol was carried out on compounds **4d,e** with an ethoxycarbonyl group in position 6 of the bicycle. The best results for the aromatization of the dihydropyrimidine fragment (products **8a,c**) were obtained when the starting compounds were heated with phenyliododiacetate in acetic acid. Some attempts to do the same aromatization with bromine in acetic acid have been ineffective so far, as they led to the formation of a mixture of products that were difficult to identify.

*General procedure for the preparation of compounds (4).* A mixture of acetylacetone (**2a**) (0.10 ml, 1.0 mmol) or acetoacetic ester (**2b**) (0.15 ml, 1.1 mmol), arylglyoxal hydrate (**1**) (1.0 mmol), and 3-aminotriazole (**3**) (0.08 g, 1.0 mmol) in 5 ml of EtOH was refluxed for 1.5–2 hour. The reaction mixture was cooled; the precipitate was filtered off, washed with EtOH, and recrystallized from EtOH.

*1-(7-Benzoyl-5-methyl-4,7-dihydro-[1,2,4]triazolo[1,5-a]pyrimidin-6-yl)ethan-1-one (4a).* Yield 271 mg (87 %), white crystals, mp 197–200 °C. <sup>1</sup>H NMR spectrum, δ, ppm: 10.95 (s, 1H, NH), 8.14 (d, *J* = 8.0; 2H, Ph), 7.72 (s, 1H, 2-H), 7.58–7.65 (m, 3H, Ph), 6.75 (s, 1H, 7-H), 2.48 (s, 3H, CH<sub>3</sub>), 2.33 (s, 3H, CH<sub>3</sub>). Found, %: C 63.77 H 4.90 N 19.76. C<sub>15</sub>H<sub>14</sub>N<sub>4</sub>O<sub>2</sub>. Calculated, %: C 63.82 H 5.00 N 19.85.

*1-[7-(4-Chlorobenzoyl)-5-methyl-4,7-dihydro[1,2,4]triazolo[1,5-a]pyrimidin-6-yl]ethan-1-one (4b).* Yield 292 mg (92 %), white crystals, mp 200–202 °C. <sup>1</sup>H NMR spectrum, δ, ppm: <sup>1</sup>H NMR spectrum, δ, ppm: 10.97 (s, 1H, NH), 8.17 (d, *J* =

8.2 Hz, 2H, H Ar), 7.72 (s, 1H, 2-H), 7.65 (d,  $J$  = 8.2 Hz, 2H, H Ar), 6.72 (s, 1H, 7-H), 2.50 (s, 3H, CH<sub>3</sub>), 2.34 (s, 3H, CH<sub>3</sub>). Found, %: C 56.79 H 4.17 N 17.80. C<sub>15</sub>H<sub>13</sub>ClN<sub>4</sub>O<sub>2</sub>. Calculated, %: C 56.88 H 4.14 N 17.69.

1-[7-(4-Bromobenzoyl)-5-methyl-4,7-dihydro[1,2,4]triazolo[1,5-a]pyrimidin-6-yl] ethan-1-one (4c). Yield 240 mg (67%), white crystals, mp 202-203 °C. Lit. mp 202-204 °C [18].

Ethyl 7-benzoyl-5-methyl-4,7-dihydro[1,2,4]triazolo[1,5-a]pyrimidine-6-carboxylate (4d). Yield 206 mg (73 %), white crystals, mp 204-206 °C. <sup>1</sup>H NMR spectrum,  $\delta$ , ppm: 10.91 (s, 1H, NH), 8.15 (d,  $J$  = 7.6 Hz, 2H, Ph), 7.70 (s, 1H, 2-H), 7.59-7.65 (m, 3H, Ph), 6.89 (s, 1H, 7-H), 3.85 (q,  $J$  = 7.2 Hz, 2H, CH<sub>2</sub>), 2.43 (s, 3H, CH<sub>3</sub>), 0.76 (t,  $J$  = 7.2 Hz, 3H, CH<sub>3</sub>). Found, %: C 61.70 H 5.10 N 17.86. C<sub>16</sub>H<sub>16</sub>N<sub>4</sub>O<sub>3</sub>. Calculated, %: C 61.53 H 5.16 N 17.94.

Ethyl 7-(4-chlorobenzoyl)-5-methyl-4,7-dihydro[1,2,4]triazolo[1,5-a]pyrimidine-6-carboxylate (4e). Yield 309 mg (89 %), white crystals, mp 203-205 °C. <sup>1</sup>H NMR spectrum,  $\delta$ , ppm: 10.98 (s, 1H, NH), 8.16 (d,  $J$  = 8.0 Hz, 2H, Ar), 7.87 (d,  $J$  = 8.0 Hz, 2H, Ar), 7.77 (s, 1H, 2-H), 6.92 (s, 1H, 7-H), 3.93 (q,  $J$  = 7.1 Hz, 2H, CH<sub>2</sub>), 2.47 (s, 3H, CH<sub>3</sub>), 0.86 (t,  $J$  = 7.1 Hz, 3H, CH<sub>3</sub>). Found, %: C 55.51 H 4.43 N 16.30. C<sub>16</sub>H<sub>15</sub>ClN<sub>4</sub>O<sub>2</sub>. Calculated, %: C 55.42 H 4.36 N 16.16.

General procedure for the preparation of compounds 5a,c,e. 1.3 mmol of acetane hydride was added to a solution of derivatives 4 (1 mmol) in 6 ml of dry pyridine in an ice bath in an argon atmosphere. The solution was left to warm to room temperature and left mixing overnight. The solution was poured into the 10 equiv. of ice, the precipitate was filtrated and purified by flash column chromatography on silica gel 60 (AcOEt/hexane 1:1).

1,1'-(7-benzoyl-5-methyl-[1,2,4]triazolo[1,5-a]pyrimidine-4,6(7H)-diyl)bis(ethan-1-one) (5a). Yield 230 mg (68 %), white precipitate, mp 207-210 °C. <sup>1</sup>H NMR spectrum,  $\delta$ , ppm: 8.30 (s, 1H, 2-H), 8.13 (d,  $J$  = 8.0 Hz, 2H, Ph), 7.57-7.72 (m, 3H, Ph), 6.64 (s, 1H, 7-H), 2.74 (s, 3H, CH<sub>3</sub>), 2.50 (s, 3H, CH<sub>3</sub>), 2.24 (s, 3H, CH<sub>3</sub>). Found, %: C 62.88 H 4.90 N 17.35. C<sub>17</sub>H<sub>16</sub>N<sub>4</sub>O<sub>3</sub>. Calculated, %: C 62.95 H 4.97 N 17.27.

1,1'-(7-(4-bromobenzoyl)-5-methyl-[1,2,4]triazolo[1,5-a]pyrimidine-4,6(7H)-diyl)bis(ethan-1-one) (5c). Yield 286 mg (71 %), white precipitate, mp 213-216 °C. <sup>1</sup>H NMR spectrum,  $\delta$ , ppm: 8.34 (s, 1H, 2-H), 8.10 (d,  $J$  = 7.6 Hz, 2H, Ar), 7.68 (d,  $J$  = 7.6 Hz, 2H, Ar), 6.67 (s, 1H, 7-H), 2.59 (s, 6H, 2CH<sub>3</sub>), 2.18 (s, 3H, CH<sub>3</sub>). Mass spectrum,

$m/z$  ( $I_{\text{rel}}$ , %): 403.0303 [M+H]<sup>+</sup> [C<sub>17</sub>H<sub>15</sub>BrN<sub>4</sub>O<sub>3</sub>]<sup>+</sup> (100), 405.0381 [M+H]<sup>+</sup> [C<sub>17</sub>H<sub>15</sub>BrN<sub>4</sub>O<sub>3</sub>]<sup>+</sup> (98).

Ethyl 4-acetyl-7-(4-chlorobenzoyl)-5-methyl-4,7-dihydro[1,2,4]triazolo[1,5-a]pyrimidine-6-carboxylate (5e). Yield 253 mg (65 %), white precipitate, mp 208-212 °C. <sup>1</sup>H NMR spectrum,  $\delta$ , ppm: 8.36 (s, 1H, 2-H), 8.15 (d,  $J$  = 7.6 Hz, 2H, Ar), 7.70 (d,  $J$  = 7.6 Hz, 2H, Ar), 6.68 (s, 1H, 7-H), 4.42 (q,  $J$  = 7.2, 2H, CH<sub>2</sub>), 2.65 (s, 3H, CH<sub>3</sub>), 2.08 (s, 3H, CH<sub>3</sub>), 1.33 (t,  $J$  = 7.2 Hz, 3H, CH<sub>3</sub>). Found, %: C 55.68 H 4.37 N 14.31. C<sub>18</sub>H<sub>17</sub>ClN<sub>4</sub>O<sub>4</sub>. Calculated, %: C 55.61 H 4.41 N 14.41.

Synthesis of 1-(7-(4-chlorobenzoyl)-4,5-dimethyl-4,7-dihydro[1,2,4]triazolo[1,5-a]pyrimidin-6-yl)ethan-1-one (6). Sodium hydride (60% dispersion in mineral oil) was added to a solution of compound 4b in DMF under argon atmosphere, and the mixture stirred at room temperature for 1 h. MeI was added dropwise and stirring continued for another 5 h. The mixture was poured into saturated aqueous NaCl (5 mL) and extracted with EtOAc (4×3 mL). The combined organic extracts were washed with saturated aqueous NaCl solution (2×8 mL) and dried over Na<sub>2</sub>SO<sub>4</sub>. The drying agent was filtered, and the solvent removed under reduced pressure to afford the product.

Yield 221 mg (67 %), yellow oil. <sup>1</sup>H NMR spectrum,  $\delta$ , ppm: 8.16 (d,  $J$  = 8.0 Hz, 2H, Ar), 7.76 (s, 1H, 2-H), 7.66 (d,  $J$  = 8.0 Hz, 2H, Ar), 6.74 (s, 1H, 7-H), 3.56 (s, 3H, NCH<sub>3</sub>), 2.57 (s, 3H, CH<sub>3</sub>), 2.36 (s, 3H, CH<sub>3</sub>). <sup>13</sup>C NMR spectrum,  $\delta$ , ppm: 195.9, 195.6, 150.6, 150.2, 149.7, 138.9, 135.1, 131.2 (2C), 129.3 (2C), 110.3, 57.7, 33.6, 31.6, 17.6. Found, %: C 58.18 H 4.44 N 16.99. C<sub>16</sub>H<sub>15</sub>ClN<sub>4</sub>O<sub>2</sub>. Calculated, %: C 58.10 H 4.57 N 16.94.

General procedure for the preparation of compounds (7d,e). Sodium borohydride (10 mmol) was added to a solution of compounds 4 (1 mmol) in 5 mL of MeOH in ice bath. After gas evolution stopped, the reaction mixture was refluxed for 1 hour. A white precipitate was formed, filtrated, and washed with MeOH.

Ethyl 7-(hydroxy(phenyl)methyl)-5-methyl-4,7-dihydro[1,2,4]triazolo[1,5-a]pyrimidine-6-carboxylate (7d). Yield 238 mg (76 %), white precipitate, mp 250-253 °C. <sup>1</sup>H NMR spectrum,  $\delta$ , ppm: 10.23 (s, 1H, NH), 7.57 (s, 1H, 2-H), 7.16-7.27 (m, 2H, Ph), 7.00-7.08 (m, 3H, Ph), 5.58 (s, 1H, OH), 5.52 (d,  $J$  = 3.0 Hz, 1H, 8-H), 4.78 (d,  $J$  = 3.0 Hz, 1H, 7-H), 4.16 (q,  $J$  = 7.0 Hz, 2H, CH<sub>2</sub>), 2.25 (s, 3H, CH<sub>3</sub>), 1.30 (t,  $J$  = 7.0 Hz, 3H, CH<sub>3</sub>).



Mass spectrum,  $m/z$  ( $I_{\text{rel}}$ , %): 313.1205  $[M+H]^+$   $[C_{16}H_{18}N_4O_3]^+$  (100).

*Ethyl 7-((4-chlorophenyl)(hydroxy)methyl)-5-methyl-4,7-dihydro-[1,2,4]triazolo[1,5-a]pyrimidine-6-carboxylate (7e)*. Yield 252 mg (73 %), white precipitate, mp 246-249 °C.  $^1H$  NMR spectrum,  $\delta$ , ppm: 10.31 (s, 1H, NH), 7.59 (s, 1H, 2-H), 7.31 (d,  $J$  = 8.0 Hz, 2H, Ar), 7.07 (d,  $J$  = 8.0 Hz, 2H, Ar), 5.72 (s, 1H, OH), 5.50 (d,  $J$  = 3.0 Hz, 1H, 8H), 4.79 (d,  $J$  = 3.0 Hz, 1H, 7-H), 4.17 (q,  $J$  = 7.0 Hz, 2H), 2.27 (s, 3H,  $CH_3$ ), 1.30 (t,  $J$  = 7.1 Hz, 3H,  $CH_3$ ). Found, %: C 55.18 H 4.88 N 16.19.  $C_{16}H_{17}ClN_4O_3$ . Calculated, %: C 55.10 H 4.91 N 16.06.

*General procedure for the preparation of compounds (8a,c)*. 1.25 equiv of  $PhI(OAc)_2$  was added to a suspension of derivatives 4 (1 mmol) in 5 mL of acetic acid. The reaction mixture was heated on oil bath at 130°C for 4 h. Another 0.5 equiv. of  $PhI(OAc)_2$  was added to the resulting solution, and stirred for 30 min. 7 mL of EtOH was added to the reaction mixture and stirred for 15 minutes more. The resulting solution was concentrated under reduced pressure. 5 mL of *n*-heptane was added and evaporated again. The residue was purified using flash-chromatography on silica gel 60 (DCM/MeOH 97:3) to give the desirable product.

*1-(7-benzoyl-5-methyl-[1,2,4]triazolo[1,5-a]pyrimidin-6-yl)ethan-1-one (8a)*. Yield 199 mg (71 %), white precipitate, mp > 300 °C.  $^1H$  NMR spectrum,  $\delta$ , ppm: 8.36 (s, 1H, 2-H), 8.12 (d,  $J$  = 8.0 Hz, 2H, Ph), 7.60-7.67 (m, 3H, Ph), 2.78 (s, 3H,  $CH_3$ ), 2.51 (s, 3H,  $CH_3$ ). Mass spectrum,  $m/z$  ( $I_{\text{rel}}$ , %): 281.1035  $[M+H]^+$   $[C_{15}H_{12}N_4O_2]^+$  (100).

*1-(7-(4-bromobenzoyl)-5-methyl-[1,2,4]triazolo[1,5-a]pyrimidin-6-yl)ethan-1-one (8c)*. Yield 266 mg (74 %), white precipitate, mp > 300 °C.  $^1H$  NMR spectrum,  $\delta$ , ppm: 8.36 (s, 1H, 2-H), 8.10 (d,  $J$  = 7.8 Hz, 2H, Ar), 7.62 (d,  $J$  = 7.8 Hz, 2H, Ar), 2.79 (s, 3H,  $CH_3$ ), 2.53 (s, 3H,  $CH_3$ ). Found, %: C 49.98 H 3.00 N 15.42.  $C_{15}H_{11}BrN_4O_2$ . Calculated, %: C 50.16 H 3.09 N 15.60.

*Molecular docking setup*. The crystallographic structure of SIRT2 co-crystallized with inhibitor SirReal2 (PDB ID: 4RMG [19]) was used for modelling a receptor. The Graphical User Interface of the AutoDock Tools (ADT) was employed to prepare the protein and ligands. The inhibitor molecule was removed while co-factor  $NAD^+$  was preserved for the docking calculations. A grid box was centered at the substrate binding pocket [17] with Cartesian

coordinates  $x$ = -16.76,  $y$ =-26.19, and  $z$ = 14.61, respectively. A receptor grid box was 40×40×40 Å with a grid spacing of 0.375 Å. The AutoDock Vina 1.1.2 software was utilized for molecular docking calculations [20-21]. The structure of the SIRT2 receptor was kept rigid throughout the docking process, while the ligand molecules were conformationally flexible. The exhaustiveness parameter was set to 164. For each docking run, nine docking poses were selected and ranked based on their score values in kcal/mol. Interaction analysis was performed using VMD 1.9.3 [22]. The pose with the lowest binding energy or binding affinity was used for further analysis.

### 3. Results and discussion

*Synthesis*. The 7-aryl[1,2,4]triazolo[1,5-a]pyrimidine derivatives 4a-e were synthesized by three-component condensation (Scheme 2). The products 5a,c,e, 6,7d,e, and 8a,c were obtained according to the corresponding reaction shown in Scheme 3.  $^1H$  NMR spectra, mass spectrometry, and elemental analysis confirmed the structure of the new compounds.

*Molecular Docking Calculations*. The structure of the human SIRT2 from Protein Data Bank (PDB ID: 4RMG) was obtained by X-ray method at a resolution of 1.88 Å [19]. The crystal structure of SIRT2 contains co-crystallized inhibitor SirReal2 (Scheme 1 and Figure 1). More co-crystal structures with other ligands and inhibitors have also become available, providing a unique opportunity to identify the substrate-binding pocket and inhibitor binding position at the molecular level [13, 16]. Therefore, several docking studies have already used this X-ray structure [13, 23]. The substrate pocket of the enzyme is also occupied by the  $NAD^+$  co-factor (green), which plays a crucial role in the enzyme's activity.

First, to test whether our molecular docking approach is able to correctly reproduce the binding mode of the co-crystallized inhibitor SirReal2, we re-docked it against the corresponding crystal structure of SIRT2. The insert in Figure 1 shows that the re-docked position of SirReal2 overlaps well with its position in the co-crystallized protein-ligand complex. The binding affinity of SirReal2 was found to be -12.0 kcal/mol, which can now be considered as some reference affinity for comparison with other studied ligands.

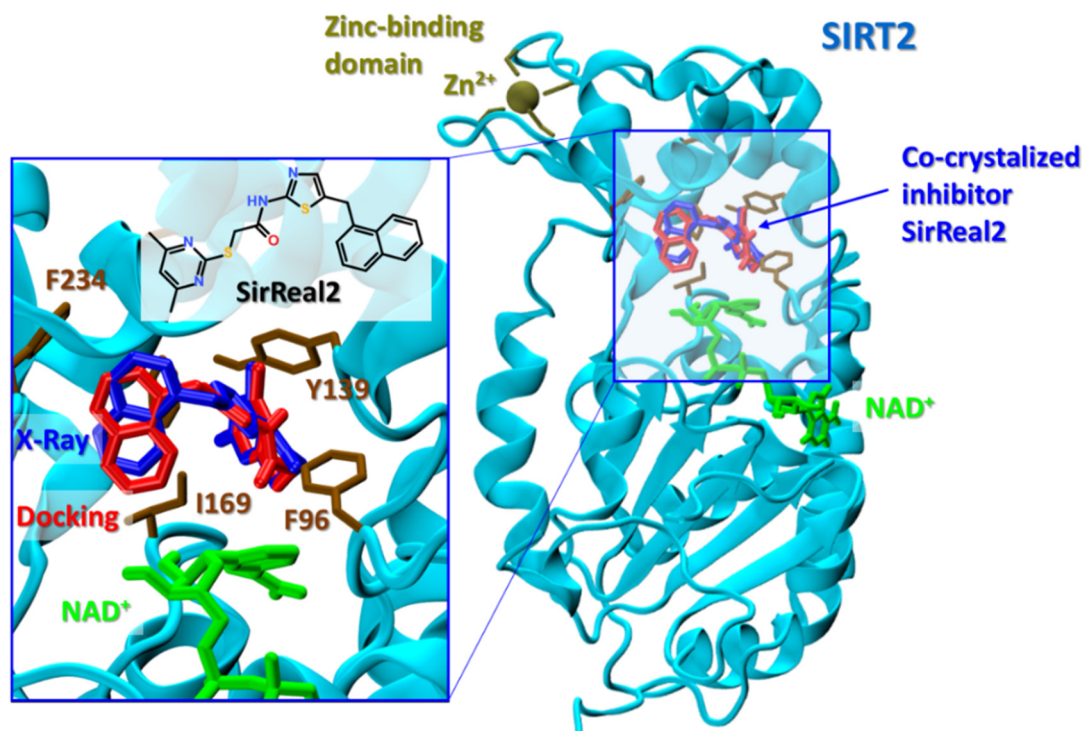


Fig. 1. The 1.88 Å X-ray structure of the human SIRT2 (PDB ID: 4RMG) [19] co-crystallized with inhibitor SirReal2 is shown by the stick representation and colored blue. The substrate pocket of the enzyme is also occupied by the cofactor  $\text{NAD}^+$  (green). Coordinated  $\text{Zn}^{2+}$  ion is located in the Zinc binding domain. The Insert: Re-docking of inhibitor SirReal2 (red) demonstrate good overlap with its X-ray position (blue).

Next, the molecular docking calculations of the studied derivatives against SIRT2 were carried out using the same docking setup. Fig. 2 shows the structure of SIRT2: ligand complexes for some derivatives that exhibit the strong binding affinity. We found that 7-aryl-triazolo[1,5-a]pyrimidine derivatives and their modified analogs bind to the enzyme hydrophobic pocket and mainly form hydrophobic interactions with a set of hydrophobic residues, such as F96, Y139, I169, and F190, respectively. These enzyme residues played a crucial role in selective recognition of other highly potent inhibitors, such as SirReal2 (Figure 1), SR86, and L1-L2 [13, 17, 23-25]. The predicted binding affinities of all studied ligands are summarized in Table 1.

Figures 2a-b demonstrate the binding modes of the two best binding ligands, **5a** and **5e**. Even though these ligands showed similar binding affinities of -8.7 and 8.3 kcal/mol, their binding conformation differed essentially. Ligand **5a** is deeply buried in the SIRT2 substrate pocket, whereas ligand **5e** is bound differently. In the SIRT2:**5e** complex, the terminal aryl ring faces outward from the substrate pocket. It suggests that the binding selectivity of the studied li-

Table 1. The binding affinity of the studied derivatives and some existing inhibitors against the SIRT2 enzyme estimated by molecular docking calculations

Ligand	Docking Binding Affinity (kcal/mol)
<b>4a</b>	-8.0
<b>4b</b>	-8.3
<b>4c</b>	-8.0
<b>4e</b>	-7.8
<b>5a</b>	-8.7
<b>5c</b>	-8.7
<b>5e</b>	-8.3
<b>6</b>	-8.0
<b>7e</b>	-7.9
<b>8a</b>	-8.3
<b>SirReal1</b>	-10.6
<b>SirReal2</b>	-12.0
<b>SR86</b>	-11.2
<b>L1</b>	-10.3
<b>L2</b>	-12.0

gands is primarily determined by interacting and recognizing the triazolo[1,5-a]pyrimidine moiety.

Table 1 shows that the studied ligands bind to the SIRT2 enzyme with affinities from -7.8



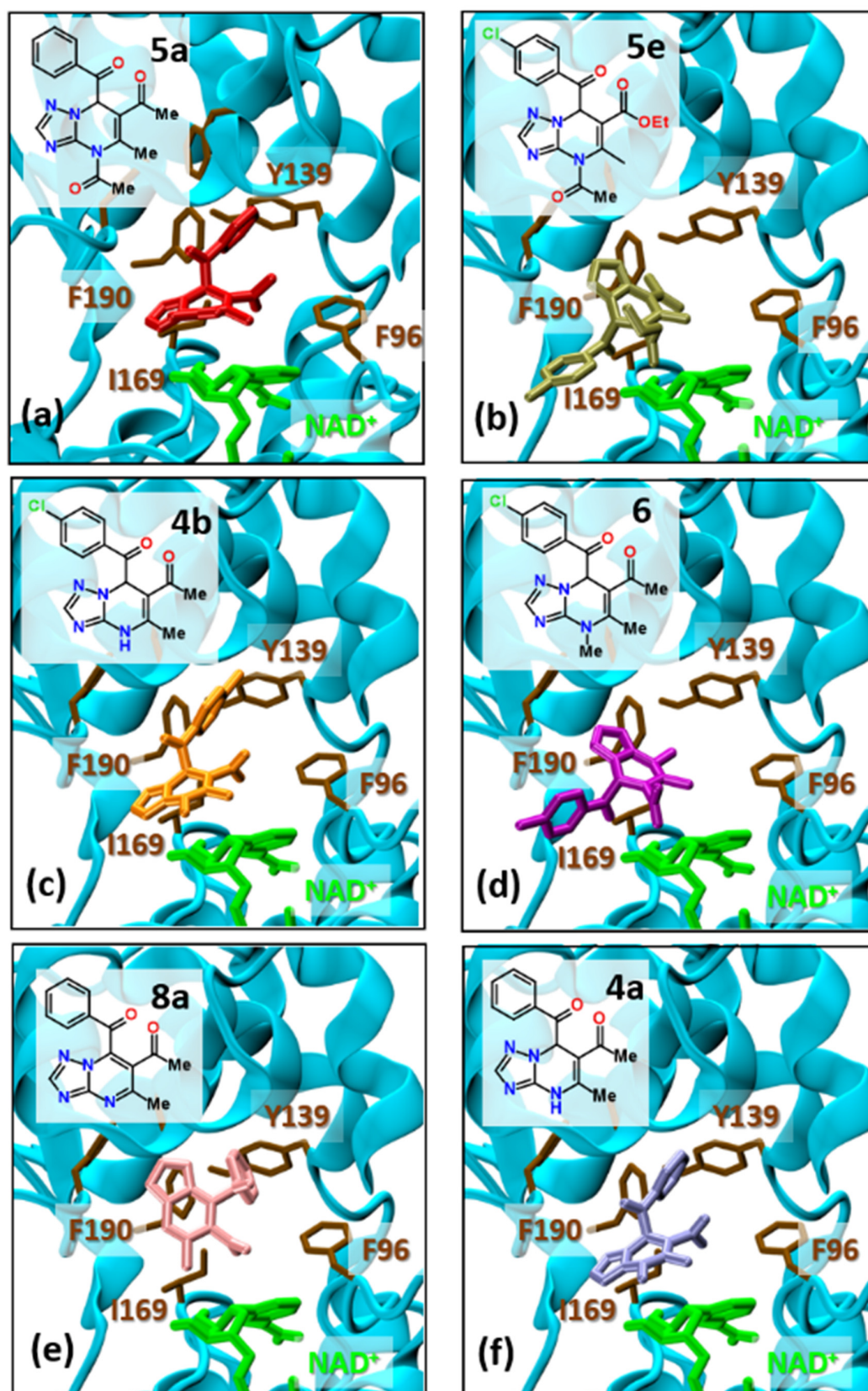


Fig. 2. The predicted binding mode of the best binding ligands with SIRT2 (PDB entry 4RMG). The ligands **5a** (a), **5e** (b), **4b** (c), **6** (d), **8a** (e) and **4a** (f) are shown by the color-coded stick representation. The cofactor NAD<sup>+</sup> located in the substrate pocket is also shown green. Some key enzyme residues are highlighted by brown.

up to 8.7 kcal/mol, respectively. Compared to the current landscape of SIRT2 inhibitors (Scheme 1), the studied ligands demonstrate the smaller binding affinities by 1-2 kcal/mol only. Thus, given their high selectivity for the SIRT2 enzyme, their inhibitory activity would be expected to be in the mM range.

#### 4. Summary

The discovery of new SIRT2 inhibitors promises therapeutic treatment for a wide range of tumors. Therefore, developing new agents and optimization of available scaffolds are still required. This work presents the synthesis and structure characterization of a series of 7-aryl-triazolo[1,5-a]pyrimidine derivatives and their post-modified analogs by the active functional groups of the bicyclic structure. The inhibitory activity and binding mechanism of the studied derivatives against the SIRT2 enzyme were considered by molecular docking calculations. We found that the functionalization of the nitrogen atom and the oxidation and reduction of the dihydropyrimidine fragment resulted in some increase in the inhibitory activity against sirtuin-2; thus, the high selectivity and affinity of N-acyl derivatives **5a,c,e** open up prospects for the development of promising anticancer drugs.

#### References

1. A. Chalkiadaki, L. Guarente. *Nat. Rev. Cancer* **15**, 608-624 (2015). <https://doi.org/10.1038/nrc3985>.
2. S.-I. Imai, L. Guarente. *Trends Cell Biol.* **24**, 464-471 (2014). <https://doi.org/10.1016/j.tcb.2014.04.002>.
3. R. Machado de Oliveira, J. Sarkander, A. G. Kazantsev, T. F. Outeiro. *Front. Pharmacol.* **3**, 82 (2012). <https://doi.org/10.3389/fphar.2012.00082>.
4. S. Chowdhury, S. Sripathy, A. A. Webster, A. Park, U. Lao, J. H. Hsu, T. Loe, A. Bedalov, J. A. Simon. *Molecules* **25**, 455 (2020). <https://doi.org/10.3390/molecules25030455>.
5. L. M. McGlynn, S. Zino, A. I. MacDonald, J. Curle, J. E. Reilly, Z. M. A. Mohammed, D. C. McMillan, E. Mallon, A. P. Payne, J. Edwards, P. G. Shiels. *Eur. J. Cancer* **50**, 290-301 (2014). <https://doi.org/10.1016/j.ejca.2013.10.005>.
6. H.-S. Kim, A. Vassilopoulos, R.-H. Wang, T. Lahusen, Z. Xiao, X. Xu, C. Li, Timothy D. Veenstra, B. Li, H. Yu, J. Ji, Xin W. Wang, S.-H. Park, Yong I. Cha, D. Gius, C.-X. Deng. *Cancer Cell* **20**, 487-499 (2011). <https://doi.org/10.1016/j.ccr.2011.09.004>.
7. C.-A. J. Ong, J. Shapiro, K. S. Nason, J. M. Davison, X. Liu, C. Ross-Innes, M. O'Donovan, W. N. M. Dinjens, K. Biermann, N. Shannon, S. Worster, L. K. E. Schulz, J. D. Luketich, B. P. L. Wijnhoven, R. H. Hardwick, R. C. Fitzgerald. *J. Clin. Oncol.* **31**, 1576-1582 (2013). <https://doi.org/10.1200/JCO.2012.45.9636>.
8. P. Y. Liu, N. Xu, A. Malyukova, C. J. Scarlett, Y. T. Sun, X. D. Zhang, D. Ling, S. P. Su, C. Nelson, D. K. Chang, J. Koach, A. E. Tee, M. Haber, M. D. Norris, C. Toon, I. Rومان, C. Xue, B. B. Cheung, S. Kumar, G. M. Marshall, A. V. Biankin, T. Liu. *Cell Death Different.* **20**, 503-514 (2013). <https://doi.org/10.1038/cdd.2012.147>.
9. A. Deng, Q. Ning, L. Zhou, Y. Liang. *Sci. Rep.* **6**, 27694 (2016). <https://doi.org/10.1038/srep27694>.
10. G. Hoffmann, F. Breitenbücher, M. Schuler, A. E. Ehrenhofer-Murray. *J. Biol. Chem.* **289**, 5208-5216 (2014). doi:10.1074/jbc.M113.487736.
11. H. Cui, Z. Kamal, T. Ai, Y. Xu, S. S. More, D. J. Wilson, L. Chen. *J. Med. Chem.* **57**, 8340-8357 (2014). <https://doi.org/10.1021/jm500777s>.
12. A. B. Penteado, H. Hassanie, R. A. Gomes, F. d. Silva Emery, G. H. Goulart Trossini. *Future Med. Chem.* **15**, 291-311 (2023). <https://doi.org/10.4155/fmc-2022-0253>.
13. W. Yang, W. Chen, H. Su, R. Li, C. Song, Z. Wang, L. Yang. *RSC Adv.* **10**, 37382-37390 (2020). <https://doi.org/10.1039/D0RA06316A>.
14. S. Sundriyal, S. Moniot, Z. Mahmud, S. Yao, P. Di Fruscia, C. R. Reynolds, D. T. Dexter, M. J. E. Sternberg, E. W. F. Lam, C. Steegborn, M. J. Fuchter. *J. Med. Chem.* **60**, 1928-1945 (2017). <https://doi.org/10.1021/acs.jmedchem.6b01690>.
15. N. A. Spiegelman, I. R. Price, H. Jing, M. Wang, M. Yang, J. Cao, J. Y. Hong, X. Zhang, P. Aramsangtienchai, S. Sadhukhan, H. Lin. *ChemMedChem* **13**, 1890-1894 (2018). <https://doi.org/10.1002/cmdc.201800391>.
16. A. L. Nielsen, N. Rajabi, N. Kudo, K. Lundø, C. Moreno-Yruela, M. Bæk, M. Fontenas, A. Lucidi, A. S. Madsen, M. Yoshida, C. A. Olsen. *RSC Chem. Biol.* **2**, 612-626 (2021). <https://doi.org/10.1039/D0CB00036A>.
17. E. Roshdy, M. Mustafa, A. E.-R. Shaltout, M. O. Radwan, M. A. A. Ibrahim, M. E. Soliman, M. Fujita, M. Otsuka, T. F. S. Ali. *Eur. J. Med. Chem.* **224**, 113709 (2021). <https://doi.org/10.1016/j.ejmech.2021.113709>.
18. N. V. Chechina, N. N. Kolos, I. V. Omelchenko, V. I. Musatov. *Chem. Heterocyc. Comp.* **54**, 58-62 (2018). <https://doi.org/10.1007/s10593-018-2230-1>.
19. T. Rumpf, M. Schiedel, B. Karaman, C. Roessler, B. J. North, A. Lehotzky, J. Oláh, K. I. Ladwein, K. Schmidtkunz, M. Gajer, M. Pannek, C. Steegborn, D. A. Sinclair, S. Ger-



- hardt, J. Ovádi, M. Schutkowski, W. Sippl, O. Einsle, M. Jung. *Nat. Commun.* **6**, 6263 (2015). <https://doi.org/10.1038/ncomms7263>.
20. O. Trott, A. J. Olson. *J. Comput. Chem.* **31**, 455-461 (2010). <https://doi.org/10.1002/jcc.21334>.
21. D. S. Goodsell, M. F. Sanner, A. J. Olson, S. Forli. *Prot. Sci.* **30**, 31-43 (2021). <https://doi.org/10.1002/pro.3934>.
22. W. Humphrey, A. Dalke, K. Schulten. *J. Mol. Graphics* **14**, 33-38 (1996). [https://doi.org/10.1016/0263-7855\(96\)00018-5](https://doi.org/10.1016/0263-7855(96)00018-5).
23. M. A. A. Ibrahim, K. A. A. Abdeljawaad, E. Roshdy, D. E. M. Mohamed, T. F. S. Ali, G. A. Gabr, L. A. Jaragh-Alhadad, G. A. H. Mekhemer, A. M. Shawky, P. A. Sidhom, A. H. M. Abdelrahman. *Sci. Rep.* **13**, 2146 (2023). <https://doi.org/10.1038/s41598-023-28226-7>.
24. G. Eren, A. Bruno, S. Guntekin-Ergun, R. Cetin-Atalay, F. Ozgencil, Y. Ozkan, M. Gozelle, S. G. Kaya, G. Costantino. *J. Mol. Graph. Model.* **89**, 60-73 (2019). <https://doi.org/10.1016/j.jmgm.2019.02.014>.
25. S. Huang, C. Song, X. Wang, G. Zhang, Y. Wang, X. Jiang, Q. Sun, L. Huang, R. Xiang, Y. Hu, L. Li, S. Yang. *J. Chem. Inform. Model.* **57**, 669-679 (2017). <https://doi.org/10.1021/acs.jcim.6b00714>.